Path integration in place cells of developing rats

Tale L. Bjerknes[a,b], Nenitha C. Dagslott[a,b], Edvard I. Moser[a,b], and May-Britt Moser[a,b,1]

[a]Kavli Institute for Systems Neuroscience, Norwegian University of Science and Technology, NO-7489 Trondheim, Norway; and [b]Centre for Neural Computation, Norwegian University of Science and Technology, NO-7489 Trondheim, Norway

Contributed by May-Britt Moser, January 2, 2018 (sent for review November 1, 2017; reviewed by John L. Kubie and Mayank R. Mehta)

Place cells in the hippocampus and grid cells in the medial entorhinal cortex rely on self-motion information and path integration for spatially confined firing. Place cells can be observed in young rats as soon as they leave their nest at around 2.5 wk of postnatal life. In contrast, the regularly spaced firing of grid cells develops only after weaning, during the fourth week. In the present study, we sought to determine whether place cells are able to integrate self-motion information before maturation of the grid-cell system. Place cells were recorded on a 200-cm linear track while preweaning, post-weaning, and adult rats ran on successive trials from a start wall to a box at the end of a linear track. The position of the start wall was altered in the middle of the trial sequence. When recordings were made in complete darkness, place cells maintained fields at a fixed distance from the start wall regardless of the age of the animal. When lights were on, place fields were determined primarily by external landmarks, except at the very beginning of the track. This shift was observed in both young and adult animals. The results suggest that preweaning rats are able to calculate distances based on information from self-motion before the grid-cell system has matured to its full extent.

development | hippocampus | place cells | navigation | path integration

Place cells in the hippocampus are often thought to be formed by integration of spatial inputs from grid cells in the entorhinal cortex (1, 2). This proposal is challenged, however, by differences in the maturation rates of place cells and grid cells. Pyramidal cells in the hippocampus express well-defined place fields as soon as spatial behavior can be tested, when rat pups leave their nest around postnatal day 16 (P16) (3, 4). In contrast, adult-like grid cells with strictly periodic spatial firing patterns have not been identified in the medial entorhinal cortex until the fourth week of life (3–5). This difference in timing has been taken as evidence that place fields can be formed in the absence of inputs from mature grid cells, for example from border cells, which express adult-like firing fields from the outset during exploration in preweaning rats (5). In support of this proposal, it was reported recently that in young rats tested in an open environment, place cells are stable only near the borders of the enclosure; stability in the middle of the environment increased only at the time when grid cells began expressing adult-like periodic firing patterns, at 3–4 wk of postnatal life (6). These findings suggest that place cells rely on both grid and border cells for accurate position coding, perhaps with border cells contributing more to position coding in rats with immature and less regular grid cells than in animals with a fully developed entorhinal–hippocampal spatial representation.

The regularity of the firing fields of adult grid cells (7), and their independence of the speed and curvature of the animal's path (7), has led to the hypothesis that these cells, or cells that they interact with, enable localized firing by integrating linear and angular speed information through a process referred to as path integration (8–10). Path integration, as expressed in grid cells, and downstream in place cells, may enable the animals to estimate distance from reference positions. The computation of distance and direction of movement in grid and place cells may be supported by local speed cells, which express instantaneous linear speed (11–13), and head direction and conjunctive grid × head direction cells, which express the animal's orientation in the environment (14–16).

Firing locations of grid cells and place cells are not determined exclusively by path integration, however. Position information may be obtained also from distal landmarks, as suggested by the fact that place fields (17) as well as grid fields (18, 19) follow the location of the walls of the recording environment when the environment is stretched or compressed. This observation points to local boundaries as a strong determinant of firing location. On the other hand, other work has demonstrated that place cells fire in a predictable relationship to the animal's start location on a linear track even when the position of the starting point is shifted (20, 21). On outbound journeys, in these experiments, the firing locations of place cells on the first part of the track reflected the distance that the animal had run from the start box. When the animals came closer to the end of the track, the place cells started to fire at fixed distances from the end location, indicating that external landmarks took over the control of firing position (20, 21). These early studies could not entirely rule out olfactory cues from the start box as contributors to start box-dependent firing, but subsequent experiments, using the power of virtual reality, were able to dissociate landmarks and distance more completely (22–24). These studies demonstrated distance coding along extensive lengths of the virtual track, suggesting, together with the early studies, that place cells, and by extension grid cells, rely conjunctively on self-motion information and external cues to determine firing location, with a significant contribution of the former (22).

In the present study, we investigated the relationship between grid cells and place cells further by determining whether preweaning rats, at an age when grid cells have not developed regularly dispersed firing patterns, have place cells whose field locations depend on self-motion information. Rats ran on a linear track with variable start positions, and locations of place

Significance

The mammalian brain has neurons that specifically represent the animal's location in the environment. Place cells in the hippocampus encode position, whereas grid cells in the medial entorhinal cortex, one synapse away, also express information about the distance and direction that the animal is moving. In this study, we show that, in 2.5–3-wk-old rat pups, place cells have firing fields whose positions depend on distance travelled, despite the immature state of grid fields at this age. The results suggest that place fields can be generated from self-motion–induced distance information in the absence of fully matured grid patterns.

Author contributions: T.L.B., E.I.M., and M.-B.M. designed research; T.L.B. and N.C.D. performed research; T.L.B. analyzed data; M.-B.M. supervised the project; and T.L.B. and E.I.M. wrote the paper.

Reviewers: J.L.K., State University of New York Downstate Medical Center; and M.R.M., University of California, Los Angeles.

The authors declare no conflict of interest.

Data deposition: The data reported in this paper have been deposited in the Norstore database, https://archive.norstore.no (accession no. 10.11582/2018.00003).

[1]To whom correspondence should be addressed. Email: maybm@ntnu.no.

This article contains supporting information online at www.pnas.org/lookup/suppl/doi:10.1073/pnas.1719054115/-/DCSupplemental.

fields were determined as a function of distance from the start location as well as external landmarks. A subset of the experiments was performed in darkness to force the rats to base navigation primarily on distance estimates as they traversed the track. If place field locations are determined by distance information and some of this distance information is derived from the regular distances between grid fields, then the stability of place cell maps would be expected to be impaired in darkness below ∼4 wk of age, before grid cells reach adult levels of spatial periodicity (3, 4).

Results

Distance-dependent firing of place cells was investigated by letting rats of different ages run three trials of 10 consecutive laps on a 200-cm linear track. On each trial, the rat ran in one direction from a start wall to an end box (Fig. 1). At the end of each lap, the animal was picked up from the end box and manually placed back at the start location. On the second trial, the track was shortened to any length between 90 cm and 180 cm, using steps of 5 cm. Different track lengths were chosen for different trials, in a manner that maximized the number of track lengths in each age group. The sequence of track lengths was chosen randomly. On the third trial, the 200-cm length was reintroduced. The three-trial sequence was performed both with room lights on and in complete darkness.

The rats were implanted with a single 16-channel microdrive aimed at CA1, with the earliest implant performed at the age of P10 and most implants taking place on P14 and P15 (range P14–P23; Fig. S1). Twenty-one juvenile animals between age P17 and P34 and 10 adult animals were tested on the linear track, whereas a different group of nine juvenile (P17–P34) and five adult animals was tested in the open field.

Hippocampal cells recorded on the linear track were classified as place cells if at least three successive bins of the track (15 cm) had a firing rate that exceeded 20% of the cell's peak firing rate. Contiguous bins satisfying this criterion were defined as preliminary place fields. Final fields were determined by extending each preliminary field successively across bins from each end, proceeding until a bin was reached where the firing rate was higher than the preceding bin, or the rate was lower than 1% of the peak rate. Fields with fewer than 30 spikes were excluded from the analyses. Only place cells with firing fields satisfying the criterion on all trials were included. In the open field, cells were classified as place cells if their spatial information content (25) exceeded the 95th percentile of spatial information values for shuffled data from the first and the last trial with room lights on.

In linear-track experiments with room lights on, 68 of the 141 cells recorded in hippocampal area CA1, or 48.2%, were classified as place cells in the P17–P20 age group. On trials in darkness, 69 out of 129 cells (53.3%) were classified as place cells at P17–P20. In the P21–P27 age group, 49 out of 115 cells in light (42.6%) and 46 out of 86 cells in darkness (53.5%) passed the criterion. For P28–P34, 25 out of 98 cells (25.5%) in light and 33 out of 86 cells in darkness (38.4%) were classified as place cells. In the adult group, the fraction of place cells was comparable to that of the youngest group: 76 out of 139 (54.7%) in the illuminated condition and 53 out of 95 (55.8%) in darkness. There was a weak but significant increase in mean firing rates with age (lights on: $r = 0.302$, $P < 0.001$, $n = 218$; lights off: $r = 0.235$, $P = 0.001$, $n = 201$), and as reported previously (3, 4), place fields became progressively more stable (within-trial correlation between age and stability of place fields on even- vs. odd-numbered laps, with lights-on: $r = 0.317$, $P < 0.001$, $n = 218$; with lights off: $r = 0.163$, $P = 0.02$, $n = 201$; between-trial correlation between age and stability of place fields on trials 1 and 3, with lights on: $r = 0.533$, $P < 0.001$, $n = 218$; with lights off: $r = 0.176$, $P = 0.013$, $n = 201$). Stability was expressed as the spatial correlation between rate maps on two occasions. Firing rates were generally not significantly different between tests in light and darkness—age: $F(3, 419) = 18.1$, $P < 0.001$; illumination condition: $F(1, 419) = 0.001$, $P = 0.973$; Illumination Condition × Age Group: $F(3, 419) = 2.64$, $P = 0.05$ (ANOVA with age group and illumination condition as between-subjects factors; illumination condition was treated as a between-subjects factor because cell samples in light and darkness had little overlap).

We then asked if place fields were determined by running distance or external cues when these were put in conflict on the middle trials with new start locations. Both in young and adult animals, we observed cells with place fields at a fixed distance from the start position, regardless of track length. Cells with distance-dependent firing fields were observed with lights on as well as in darkness, but they were more pronounced in darkness, when conflicting stationary visual cues were absent (Fig. 2 *A* and *B* and Fig. S2). When lights were on, the majority of the cells fired at a fixed distance from the never-moving end box, suggesting that their firing locations depended more strongly on external cues (Fig. 2 *C* and *D* and Fig. S2). Place fields with a fixed distance from the start wall were observed only at the beginning of the short track in the lights-on condition, consistent with previous observations using a similar task in an illuminated environment (20, 21).

To determine more precisely the contribution of distance from the start wall, we constructed stacks of linear rate maps where x provides location and y indicates cell identity (Fig. 3). For these analyses, we excluded the first 20 cm and the last 10 cm of the track to rule out immediate sensory stimulation, such as touch of the start wall, as an explanation of spatial firing at the beginning of the track (P20 rats were up to 18 cm long, from nose to end of the tail). For the initial 200-cm trial, cells were sorted according to the position of the cell's first place field on the track, after exclusion of the track ends, such that place fields on the beginning of the remaining track were at the top of the matrix and place fields at the end were at the bottom (Fig. 3, *Top* rows of *A* and *B*). Rate maps for the same cells on the short track lengths were displayed separately but still with 20-cm and 10-cm cutoffs at the ends (Fig. 3, *Bottom* and *Middle* rows of *A* and *B*). When lights were on, for most of the track, the fields aligned with the end of the track, such that firing locations were similar irrespective of starting position (Fig. 3*A*). When lights were off, fields matched better the distance run from the starting position (Fig. 3*B*). However, the sequence of place fields was retained in both illumination conditions. When arranged according to the sequence of place fields on the long track, and with short tracks aligned to the position of the start wall, place fields roughly followed the same sequence as on the long track. Sequences were maintained among simultaneously recorded cells (trials with five cells or more; mean correlation between distance of peak of place field from start wall on short and long tracks ±SEM, with lights on: 0.64 ± 0.155, $t = 4.11$, $P = 0.003$, one-sample t test with $H_0 = 0$, $n = 9$; with lights off: 0.54 ± 0.140, $t = 3.86$, $P = 0.004$, one-sample t test with $H_0 = 0$, $n = 10$).

Based on these analyses, population vectors were defined for each bin of the long and short tracks based on unsmoothed

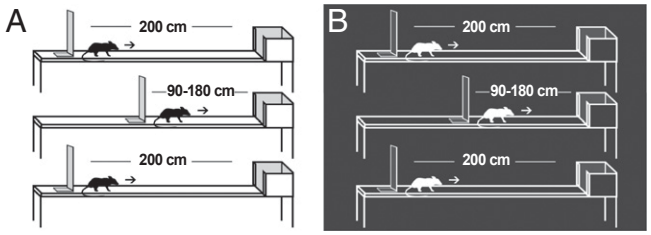

Fig. 1. Experimental setup (*A*, lights on; *B*, lights off). Rats ran in one direction from a starting wall to an end box. The length of the track was 200 cm on the first and third trials. On the second trial, length was chosen semirandomly between 90 cm and 180 cm, in 5-cm steps. Each trial consisted of 10 laps. The location of the end box was constant, whereas the location of the start wall varied with track length.

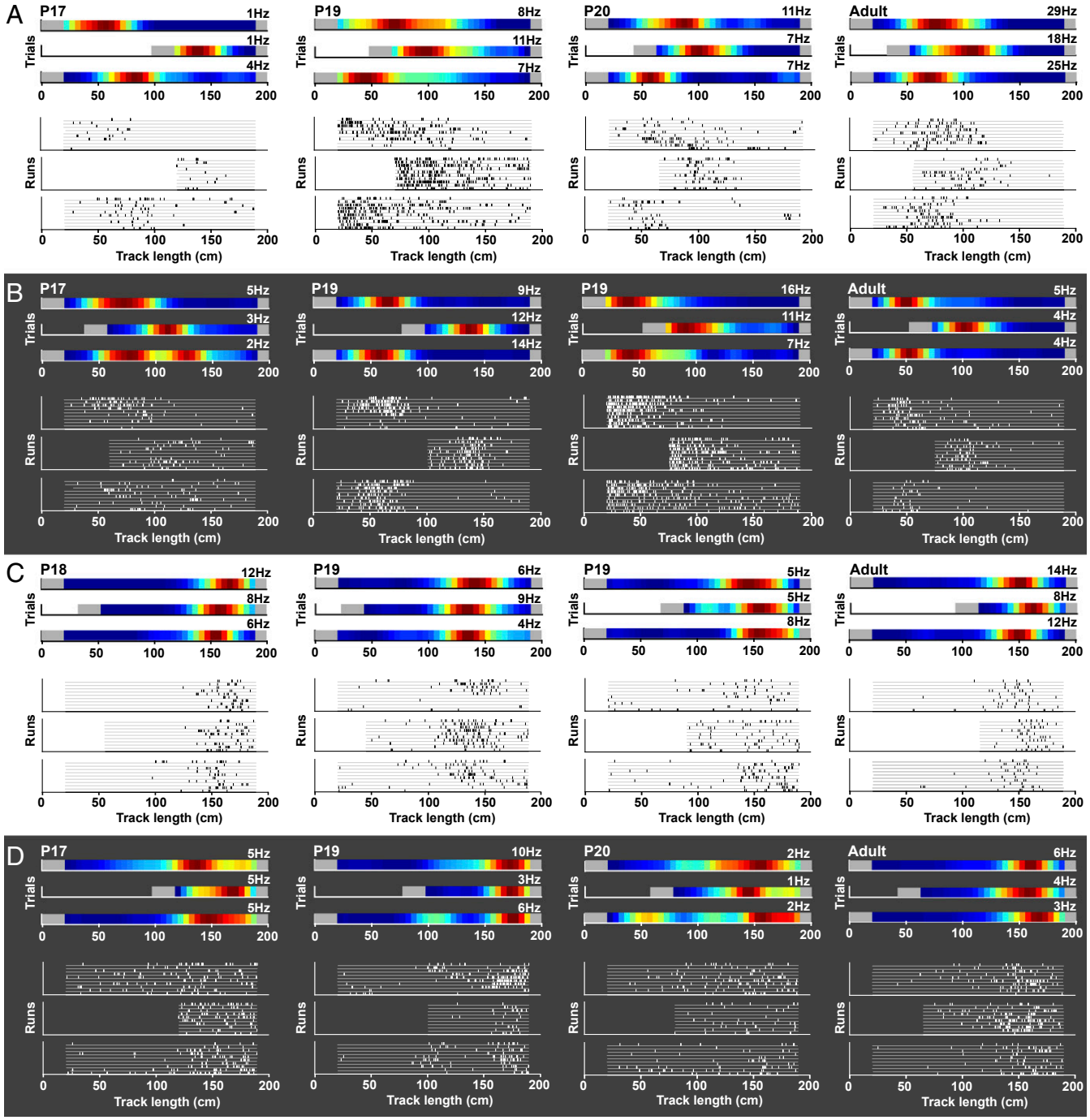

Fig. 2. Example place cells on complete and shortened tracks at P17–P20 and adult age. (*A*) Example place cells with firing fields at the beginning of the track. Cells were tested with room lights on. Rate maps are shown for each track length. Color coding is normalized, with dark red showing the cell's peak firing rate and dark blue a firing rate of 0. Below are raster plots for the same cells. Each run is marked by a gray line, and spike positions are indicated. Note that some cells with place fields near the beginning of the runway fire at fixed distances from the start wall already at P17–P20. (*B*) Similar to *A* but with room lights off. Cells fire at a fixed distance from the start wall. (*C*) Cells with place fields on the last part of the linear track. Lights were on. Fields have a fixed distance from the end box. (*D*). Similar to *C* but with lights off.

distributions of firing rates across the cell population. Population vectors across bins of the full-length track were cross-correlated with population vectors for the same cells on the short tracks, with the initial and final segments of the track excluded as before (Fig. 4). Correlations were not included in the matrix when the number of cells in the stack fell below 10 cells, which it frequently did at the right end where fewer trials contributed. If all cells fired at a fixed distance from the start wall, this should result in high correlations along the diagonal starting from the bottom left corner, from (0,0) to (t,t), referred to as the starting diagonal. For recordings with room lights on, correlations were high along the leftmost part of the starting diagonal in all age groups, but this alignment was expressed only at the very beginning of the track (Fig. 4*A*). In all groups, the approximation to the starting diagonal was more pronounced, and extended across a much wider section of the track, when the recordings were

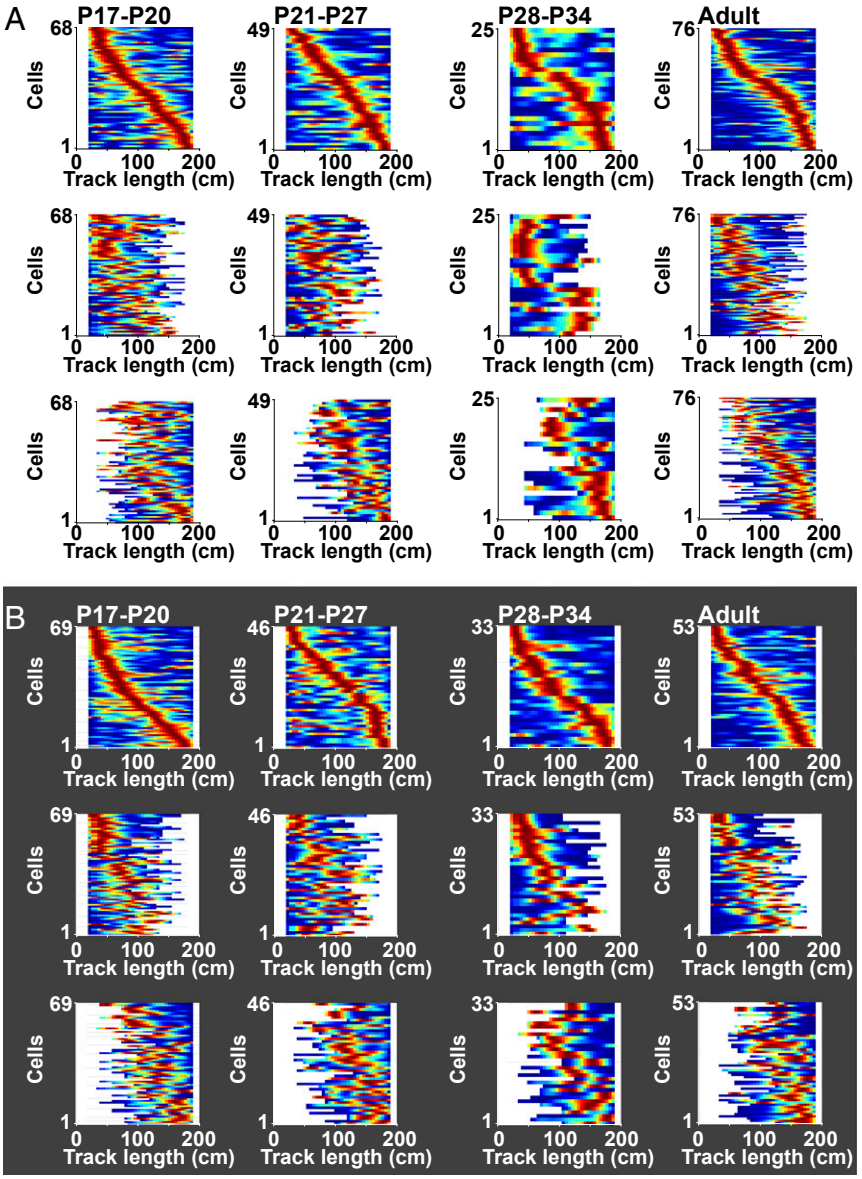

Fig. 3. Stacks of color-coded place-cell rate maps for all age groups. (*A*) Lights-on condition. Peak firing rate is dark red; firing rate of 0 is dark blue. *Top* shows place fields on first trial (200 cm), sorted by position of the first identified firing field from the left. Cell numbers are indicated to the left, on the *y* axis. *Middle* shows the same cells in the same order but for the second trial, with the short track (90–180 cm, variable start position, constant end position). Trials are aligned to start position on the track. (*Bottom*) Same as in *Middle* but with trials aligned to end position. (*B*) Lights-off condition. Layout and symbols as in *A*.

made in darkness (Fig. 4*B*). This indicates that, in pups as well as adults, place cells relied more on distance traveled when distal landmarks were no longer available.

In a subsequent analysis, the stack of place fields was aligned instead at the end position of the track (Fig. 4 *C* and *D*). Population vector correlations were determined in the same way as for trials with alignment to the start position. If all cells fired at a fixed distance from the end box, this should result in high correlations along the diagonal starting at the top right corner (end_{long}, end_{short}), referred to as the end diagonal. When room lights were on, high correlations were indeed observed along this diagonal near the top right corner of the matrix in all age groups (Fig. 4*C*), but not surprisingly this effect was reduced in darkness, although it did not disappear entirely (Fig. 4*D*). The results suggest that, in all age groups, cells use distal visual landmarks to systematically position place fields at a fixed distance from the end box when such landmarks are available.

To ensure that the differences between light and dark conditions, and the lack of differences between age groups, did not reflect differences in the size of cell samples, we also generated population vector matrices after randomly down-sampling cell numbers in each group to the number of cells in the age group with the fewest cells (25 cells with lights on; 33 cells with lights off). Down-sampling did not change the correlation pattern: With lights off, place cells depended on the distance run along the track, whereas with lights on, field locations were controlled by stationary external cues along most of the track after the initial centimeters (Fig. S3). In another control analysis, we ensured that the threshold of 30 spikes for identification of place fields did not have a major effect on the results, by repeating the population-vector cross-correlation analyses with criteria of a minimum of 20, 40, and 50 spikes per field. Changing the threshold did not change the pattern of firing fields (Fig. S4).

To quantify whether the population of recorded place cells fired systematically in a fixed relationship to either the start or the end position of the linear track (26), we performed two sets of analyses. First, we asked whether the peaks in the cross-correlation matrix for short versus long tracks exceeded chance values determined by a shuffling procedure where spikes were displaced randomly along the track for each cell. For each bin of the cross-correlation matrix, we compared the observed correlation value with the distribution of correlation values for

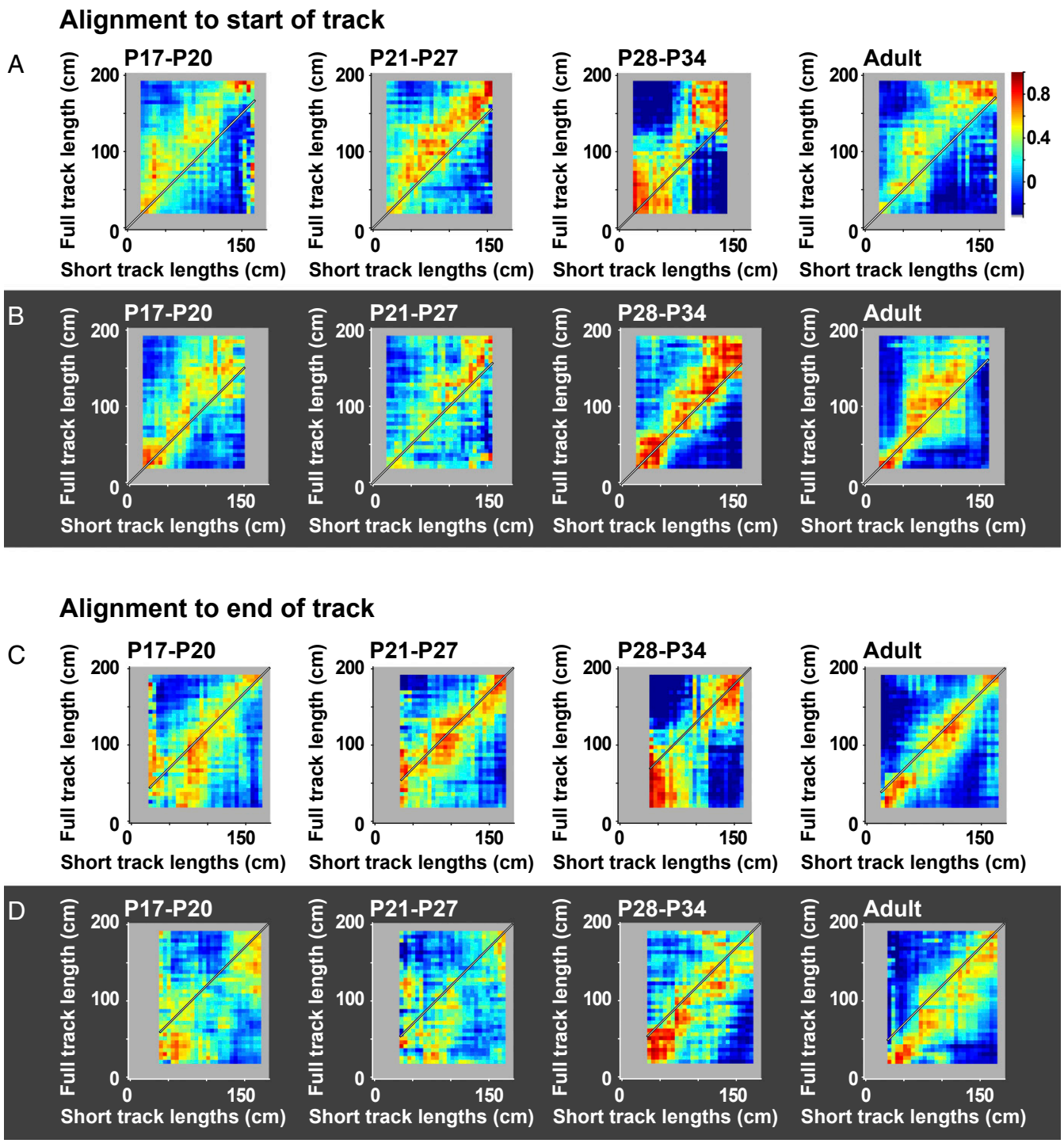

Fig. 4. Population vector cross-correlation matrices for place cells from all age groups. (*A*) Correlation matrices in lights-on condition, with vectors aligned at the start position. Positions on the full-length track are plotted on the *y* axis; positions on the short-length tracks are plotted on the *x* axis. Color-coding of pixels shows correlations between firing rates from all recorded cells in single bins of the full-length track with firing rates from all recorded cells in corresponding bins on the short-length tracks. The number of cells contributing to bins decreases from left to right on the *x* axis, reflecting the lower number of short tracks with lengths near 180 cm. The diagonal from the bottom left corner (0,0) to (t,t)—the starting diagonal—indicates where peak correlations would fall if cells fired at a fixed distance from the start wall. Note in all age groups the lack of high correlations near the starting diagonal, except at the very beginning, suggesting that, for most of the runway, place cells recorded with room lights on did not systematically fire as a function of distance from the start wall. Note also the general shift toward supradiagonal values along most of the track (after the initial centimeters), suggesting that external cues took over as determinants of firing. (*B*) Population vector correlation matrices as in *A* for all age groups in the lights-off condition. Note that, in darkness (unlike with lights on), peak correlations align with the starting diagonal in all age groups, suggesting that firing location was now determined by distance moved from the beginning of the track. (*C*) Population vector correlation matrices as in *A* but now with short lengths aligned to the end position of the track. The diagonal from the top right corner (the end diagonal) indicates where peak correlations would fall if cells fired at a fixed distance from the end box. Note high correlations in the top right corner in all groups when lights were on. (*D*) Same as *C* but with room lights off. Note lack of high correlations along the end diagonal as well as the rightward shift of high correlations compared with the diagonal, which would be expected if animals do not see the external landmarks.

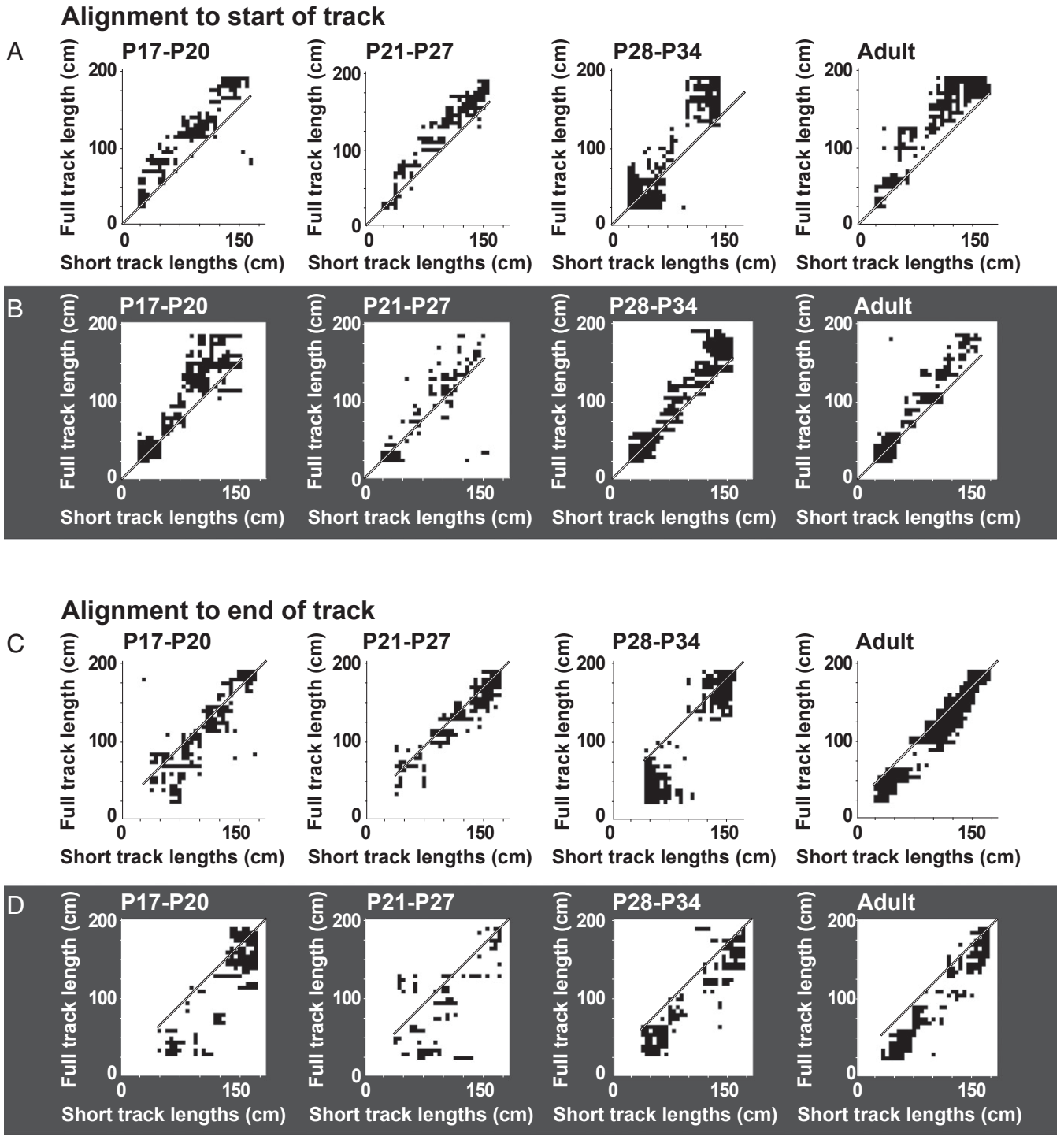

Fig. 5. Population vector cross-correlograms showing comparison between observed and shuffled data. (*A*) Population vector matrices similar to Fig. 4, with position on the full-length track on the *y* axis and position on the short-length track, aligned at the start position, on the *x* axis. Room lights were on. Diagonal from bottom left corner (starting diagonal) indicates where peak correlations would fall if place cells fired at a fixed distance from the start wall. Bins where the observation exceeded the 95th percentile of the control distribution are shown in black; remaining bins are white. Note that, except for the initial bins, peak correlations are shifted upwards in all groups, reflecting alignment not with the start wall but with the stationary cues outside the track. (*B*) Population vector matrices showing bins with correlations above the 95th percentile threshold of the shuffled data, as in *A*, but when lights were off. Note that significant correlations are still displaced to the left but cluster closer to the starting diagonal than in the lights-on condition, suggesting that place fields are now anchored more strongly to the starting point of the track. (*C*) Similar to *A* but with the short-length track aligned at the end position. Lights are on. Diagonal from the upper right corner (end diagonal) indicates where peak correlations would fall if place cells fired at a fixed distance from the end box. Note that bins with significant correlations are closer to the diagonal near the end of the track, suggesting that place cells fired with an increasingly fixed relationship to the end box and the external stationary visual cues. (*D*) Similar to *C* but in darkness. Significant correlations exhibit weaker clustering around the end diagonal than in the lights-on condition. Note also the rightward shift of high correlations, consistent with anchoring of place fields to the start position.

1,000 sets of shuffled data. In multiple bins near the diagonals of the cross-correlation matrix, the observed values exceeded the 95th percentile of the shuffled values (Fig. 5). For each of these significant bins, we determined the distance to the diagonal (positive, below diagonal; negative, above diagonal). When the short track lengths were aligned at the start position, the distance to the starting diagonal was negative regardless of whether lights were on (Fig. 5*A*)—mean ± SEM and one-sample *t* tests for $H_0 = 0$ for P17–P20: −5.17 ± 0.49, $t(31) = 10.48$; P21–P27: −4.16 ± 0.50, $t(28) = 8.41$; P28–P34: −4.72 ± 0.75, $t(32) = 6.28$; adult: −5.71 ± 0.58, $t(30) = 9.86$; all $P < 0.001$—or whether lights were off (Fig. 5*B*)—P17–P20: −4,58 ± 0.73, $t(31) = 6.28$; P21–P27: −2.66 ± 0.82, $t(27) = 3.25$; P28–P34: −3.02 ± 0.60, $t(33) = 5.06$; adult: −3.43 ± 0.55, $t(27) = 6.26$; all $P < 0.005$. However, the offset from the diagonal was significantly larger with lights on than lights off—illumination condition: $F(1, 247) = 11.2$, $P = 0.001$; ANOVA with age group and illumination condition as between-subjects factors. There was no significant effect of age group—$F(3, 247) = 2.10$, $P = 0.101$; Illumination Condition × Age Group: $F(3, 247) = 0.61$, $P = 0.612$—suggesting that in all age groups, place fields are determined more by self-motion information when lights are off and more by visual cues when lights are on.

The weaker leftward shift from the starting diagonal in the darkness condition was matched by a stronger rightward shift from the end diagonal. The offset from end diagonal was positive both for the illuminated condition (Fig. 5*C*)—P17–P20: 2.90 ± 0.74, $t(32) = 3.91$; P21–P27: 1.84 ± 0.51, $t(28) = 3.61$; P28–P34: 3.88 ± 0.95, $t(27) = 4.07$; adult: 2.17 ± 0.43, $t(31) = 5.05$; all $P \leq 0.001$—and for the darkness condition (Fig. 5*D*)—P17–P20: 6.54 ± 1.02, $t(27) = 6.39$, $P < 0.001$; P21–P27: 3.80 ± 1.43, $t(23) = 2.65$, $P = 0.014$; P28–P34: 4.11 ± 0.66, $t(30) = 6.21$, $P < 0.001$; adult: 4.86 ± 0.54, $t(29) = 9.05$, $P < 0.001$. The positive offset from the end diagonal was significantly larger with lights off than lights on, $F(1, 235) = 14.12$, $P < 0.001$. There was no significant effect of age, $F(3, 235) = 1.94$, $P = 0.124$; Illumination Condition × Age Group: $F(3, 235) = 1.65$, $P = 0.179$. Taken together, these analyses show that, across all age groups, the offset from the start diagonal is smaller, and the offset from the end diagonal larger, in the dark condition than in the light condition, as would be expected with a stronger contribution of self-motion information in the absence of visual cues.

The forward shift of place fields on start box-aligned trials, and its amplification on lights-on trials, was confirmed in a second analysis, where we determined whether and how much the distribution of correlation values in the cross-correlation matrix for long versus short tracks was displaced compared with an autocorrelation matrix generated from the short-track data alone (Fig. 6). Specifically, for each trial, we shifted the cross-correlogram for long versus short tracks in a bin-by-bin manner to obtain the displacement of the matrix along the track that yielded the maximum correlation with the autocorrelation matrix for the short track. Only the lower part of the cross-correlation matrix, corresponding to the length of the short track, was compared with the autocorrelogram (Fig. 6*A*). When lights were on, maximum correlation was obtained with a left-to-right shift of the cross-correlation matrix, compared with the autocorrelation matrix, of 7 bins (35 cm) in the P17–P20 and P21–P27 groups, 0 bins (0 cm) in the P28–P34 group, and 5 bins (25 cm) in the adult group (Fig. 6*B*). When lights were off, the displacement required to obtain maximum matrix correlation was smaller, with no displacement (0 bins) in the P17–P20 and P21–P27 groups and only 2 bins (10 cm) in the P28–P34 and adult groups (Fig. 6*C*), consistent with the darkness-induced reduction of offsets from the starting diagonal in the cross-correlation matrix (Fig. 5*B*).

If the location of the place fields was influenced by the distance the rats had moved from the start wall, this effect should, particularly in the illuminated condition, be expressed most strongly at the beginning of the track, before position had been recalibrated by external visual cues. Thus, we determined the shift between cross-correlation and autocorrelation matrices separately for the initial half of the runway, corresponding to the lower left quadrat of the matrices (Fig. 6*D*). When lights were on, maximum matrix correlation appeared with a left-to-right shift of 4 bins (20 cm) in the P17–P20 group, 3 bins (15 cm) in the P21–P27 group, and 1 bin (5 cm) in the P28–P34 and adult age group, pointing to a forward but generally smaller offset than for the matrix as a whole (Fig. 6*E*). When lights were off, maximum correlation was obtained with no displacement (0 bins) in all age groups, suggesting that the population vectors were now completely aligned with the diagonal from the starting point (Fig. 6*F*). The displacement on lights-on trials was significantly larger than on lights-off trials when the analysis was restricted to the lower left quadrants of the cross-correlation and autocorrelation matrices, $t(6) = 3.00$, $P = 0.024$ (independent-samples *t* test for four age groups). The difference did not reach significance when the full matrices were analyzed, $t(6) = 2.14$, $P = 0.076$.

Taken together, these findings suggest that, in all age groups, firing locations of place cells are determined conjunctively by distance cues and external landmarks. On the initial part of the track, place fields may be encoded by path integration almost exclusively, but when lights are on, stationary landmarks seem to take over as determinants as soon as the rats have walked a few tens of centimeters out on the runway.

Finally, we examined the stability of place fields in an open field during foraging in darkness. Rats of different postnatal ages ran in a 90 cm-wide cylinder, first with room light on, then with lights off, and then again with lights on (Fig. 7). All trials were performed in the same box in the same room. Place cells showed a slight increase in spatial information content with age, both in light and in darkness (Fig. 7*B*, correlation between age and spatial information with lights on: $r = 0.316$, $P < 0.001$, $n = 121$; lights off: $r = 0.303$, $P = 0.001$, $n = 121$). The increase in information content was accompanied by an age-related increase in mean firing rates ($r = 0.275$, $P = 0.002$, $n = 121$), which might influence the spatial information values (27). In accordance with the earlier studies, also the stability of the place cells increased as the rats grew older (Fig. 7*C*). Stability, expressed as the correlation between the first and second half of the first trial, increased significantly with age, both with lights on (correlation between stability and postnatal recording day: $r = 0.383$, $P < 0.001$, $n = 121$) and with lights off ($r = 0.493$, $P < 0.001$, $n = 121$).

Discussion

The present study confirms previous work showing that the perception of the distance that an animal has moved from a salient cue is sufficient for place cells to fire at specific locations. It extends this work by showing that, during postnatal development, such information is sufficient for place-field formation as early as place cells can be measured, before the age when grid cells have reached full functional maturity in the medial entorhinal cortex. In all age groups, at the beginning of the runway, place cells often fired at fixed distances from the starting location even when the start position was shifted. This effect increased substantially in darkness, when the mismatch between distal landmarks and start position was disguised. In darkness, the start wall could not be identified visually, and its moving location ruled out olfactory influences, leaving proprioceptive cues, and path integration, as the main source of information about how far the animal had run, at all ages.

Our recordings were performed across an age range when grid cells only have irregularly spaced firing fields (3–5). However, place cells had confined firing fields that were determined, at least in darkness, by how far the animal had moved from the start location. Our findings thus raise the possibility that regularly spaced grid patterns of the mature medial entorhinal cortex are not required for place cells to fire at fixed distances from salient landmarks on a running path. This could be taken as evidence against a role for grid cells in path integration-dependent place-cell firing in the hippocampus.

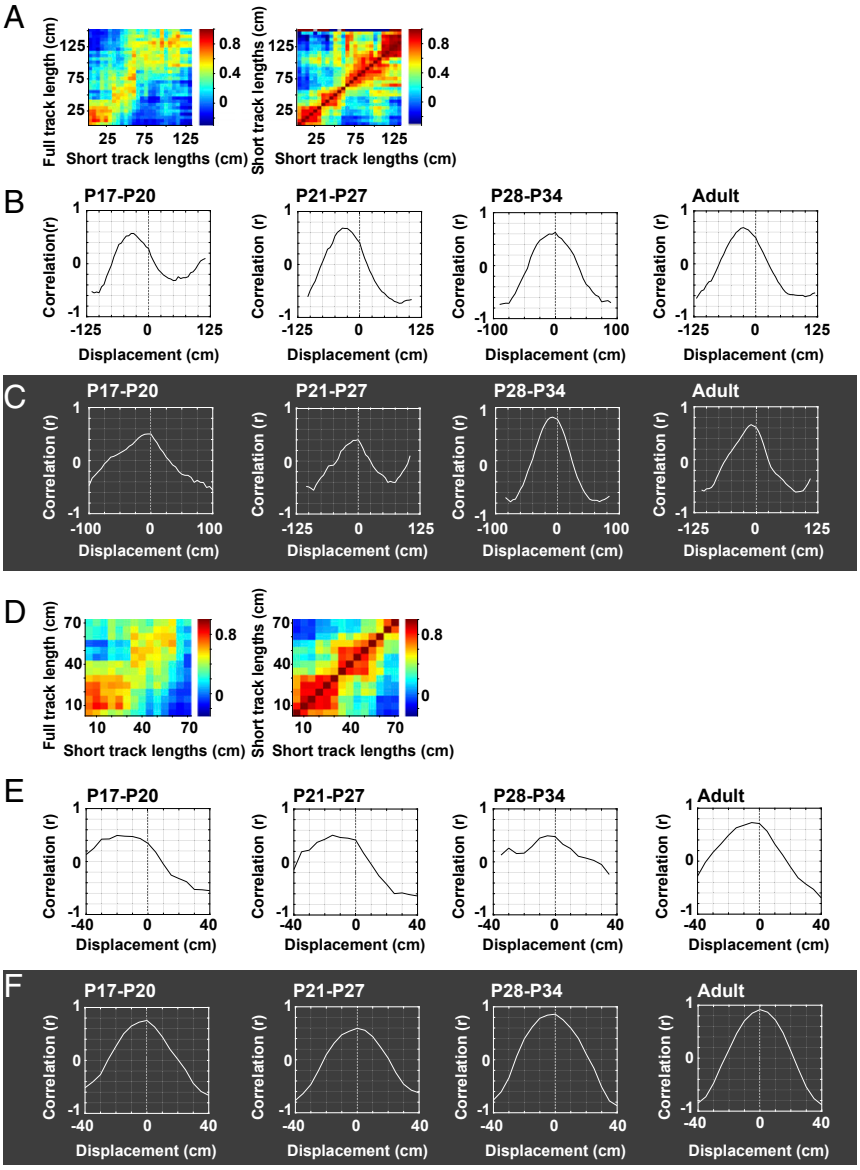

Fig. 6. Displacement of cross-correlation matrix relative to autocorrelation matrix for rate maps on the short track. (*A*) Example rate maps on long vs. short track (*Left*) and corresponding autocorrelation matrix for the short track (*Right*). For the cross-correlation matrix (from Fig. 4), only the lower part, equivalent to the length of the short track, is shown, as only this part could have overlapping data, and could be correlated with, the autocorrelation matrix. Data shown are from the P17–P20 age group tested with lights off. (*B*) Comparison of cross-correlation and autocorrelation matrices for lights-on condition. For each trial, the cross-correlation matrix (lower, overlapping part) is shifted, bin by bin, relative to the autocorrelation. Line diagrams show correlations for successive horizontal shifts of the cross-correlogram. Negative displacement values indicate that maximum correlation is obtained by shifting the cross-correlogram in a left-to-right direction compared with the autocorrelogram. Note that, except for the P28–P34 group, the correlation peaks at negative displacement values, suggesting that place fields on the short tracks were shifted forward compared with the expected location if they depended only on the starting position. (*C*) Same as in *B* but with lights off. Maximum correlation was now obtained nearer the 0 position, suggesting that fields largely remained aligned to the start of the track. Alignment with the autocorrelogram was observed in all age groups. (*D*) Lower left quadrants of cross-correlation and autocorrelation matrices (bottom left parts of matrices in *A*). (*E*) Comparison of cross-correlation and autocorrelation matrices using a stepwise shift procedure as in *B* but now for the lower left quadrant of the matrices only. Lights were on. (*F*) Same as in *E* but with lights off. Maximum correlation for the lower left quadrant of the cross-correlation and autocorrelation matrices was observed with no displacement, confirming that fields remained largely aligned to the start position in darkness. Anchoring to the start position was observed during darkness in all age groups.

One alternative possibility though is that place cells are able to encode sequences independently of position information. As rats run down the linear track, sequences may be expressed in a synfire chain-like manner irrespective of positional information reaching the hippocampus through proprioceptive senses. The observation of time cells firing at certain times from a reference time (28, 29), independently of the animal's movement (30, 31), would be consistent with such a possibility. Speaking against this possibility, the animals had well-confined place fields in the open field task, even in darkness. This would not be expected if firing fields reflected merely the activation of a chain of place cells, independently of information about the animal's trajectory, since sequences of activated place cells vary constantly in any 2D foraging task.

A second and perhaps more likely alternative, consistent with a role for grid cells at all ages, is that the weak spatial periodicity of early grid cells, when expressed in large cell ensembles, is sufficient for downstream place cells to decode position reliably. Theoretical work has shown that position can be decoded effectively from highly distorted grid patterns so long as the distortions are expressed similarly across cells of the grid module (32). Whether the dispersed firing patterns of immature grid cells contain sufficient positional information for place cells to be activated at the same confined positions on repeated trials remains an open issue that must await future studies with simultaneous recordings from larger numbers of grid cells in young animals.

Methods

Subjects. We recorded neural activity from the hippocampus in 45 Long–Evans rats. On the linear track, we recorded neural activity from 10 female and 11 male juvenile animals as well as three female and seven male adult rats. A separate group of four female and five male juvenile rats and five male adult rats was tested in the open field. Total body length including the tail at P20 was ~18 cm (15 cm from diode position to tip of the tail).

Pregnant mothers were checked multiple times per day between 8 AM and 8 PM. P0 was defined as the first day a litter was observed. Juvenile animals were kept with their mother and siblings until weaning at P21. Litter sizes did not exceed 10 pups. A maximum of four rats from each litter were implanted with microdrives and tetrodes. The pups lived with their mothers in transparent Plexiglas cages (46 cm × 40 cm × 40 cm) or in a cage with walls made of metal bars for climbing (95 cm × 63 cm × 120 cm). Both environments were enriched with fabric or plastic houses, paper as nest material, and toys. Juvenile animals had free access to food and water throughout the experiment,

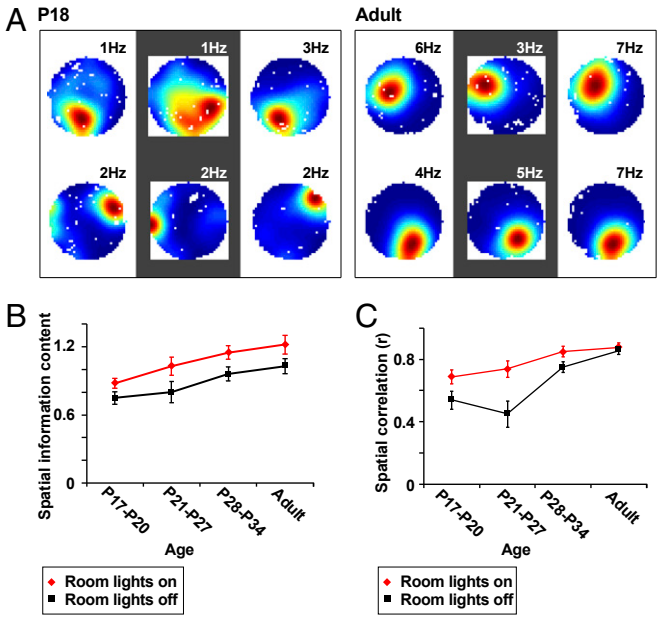

Fig. 7. Place cells in juvenile and adult animals during testing in an open environment with lights on or off. (*A*) Color-coded firing rate maps from two example place cells recorded in trials with room lights on (first and third column) and a trial with room lights off (second column) at P18 (*Left*) or adult age (*Right*). Dark red is the cell's peak firing rate; dark blue is a firing rate of 0. (*B*) Spatial information content as a function of age in first light trial (red) and the middle dark trial (black). (*C*) Within-trial correlations for first light trial (red) and the dark trial (black) for all age groups.

whereas adults were mildly food deprived. All rats were held on a 12 h light/12 h dark cycle and tested in the dark phase.

Surgery. Rat pups were implanted between P10 and P23, with most implants taking place on P14 and P15. Both pups and adult rats were implanted with a single microdrive containing four tetrodes made of 17 μm polyimide-coated platinum–iridium (90–10%) wire. Tetrodes were cut to the same level and platinum plated to impedances of ~150 kΩ at 1 kHz.

The rats were anesthetized in an induction chamber with 5% vaporized Isoflurane and 2.0 mL/min room air and then moved to a stereotactic frame with an Isoflurane level of 3% and 1.2–1.4 mL/min room air. Isoflurane was gradually reduced to 0.5–1% during the surgery. The animal received s.c. injections of bupivacaine (Marcaine) on the skull surface, as well as carprofen (Rimadyl) in pups or buphrenorphine (Temgesic) in adults as a general analgesic. Tetrodes aiming for CA1 were implanted at 3.6–3.8 mm posterior to bregma, 2.5–3.0 mm lateral to the midline, and 1.4–1.7 mm ventral to the dura. Jeweller's screws and dental cement kept the implant attached to the skull. After waking up from anesthesia, the preweaning animals were placed back with their siblings first and then with their mother and siblings.

Data Collection on the Linear Track. Data collection started the day after surgery. The rats sat on a flower pot covered with towels while the signals were checked. The implant was coupled to a recording system through a 16-channel lightweight counterbalanced cable, and the signal was passed through an AC-coupled unity-gain operational amplifier. The tetrodes were lowered in steps of 25–50 μm until single units could be isolated at appropriate depths.

Thirty-one of the animals with hippocampal implants were tested while the rats were running in one direction on a 2 m-long linear track. The track was placed 70 cm above the floor and had a width of 13 cm. A continuous dark green linoleum mat covered the length of the track. The mat had a rough surface to improve the grip for the youngest animals. The track was located at the same position in the room throughout the experiment. The start position on the track was defined by a wall behind the animal (22 cm wide, 30 cm high) and the end position as the point where the animal walked into a 26 cm × 26 cm × 26 cm box through a 11 cm-wide opening. Before each trial, the animal was placed close to the starting wall, after which it ran toward the end box, where it received a chocolate or vanilla-biscuit crumb reward (Fig. 1). Experiments were performed either with room lights on or in complete darkness, with the experimenter wearing infrared light-emitting night vision goggles.

A session consisted mostly of three trials, each including 10 laps (all trials with lights on or all with lights off). Between each lap, the animal was picked up from the end box and manually placed back at the start location. The linoleum mat was washed between each lap. On the second trial, the track was shortened from 200 cm to lengths between 90 cm and 180 cm, selecting among multiples of 5 cm. The lengths were chosen semirandomly so that most 5-cm blocks were sampled in all age groups. A subset of the animals ran two trials with shortened tracks (each consisting of 10 laps). Only the first of these was used in further analyses. On the third trial, the rat was reintroduced to the 200 cm-long track.

Recorded signals were amplified 6,000–14,000 times and bandpass-filtered between 0.8 and 6.7 kHz. Triggered spikes were stored to disk at 48 kHz with a time stamp of 32 bits. A camera in the ceiling recorded the position of one small and one large light-emitting diode (LED) on the head stage. The diodes were positioned 6 cm apart and aligned transversely to the body axis.

Analyses of Spike and Position Data on the Linear Track. To get a reliable start and end position for all 10 laps in each trial, the outermost 20 cm (4 bins) at the beginning of the track or 10 cm (2 bins) at the end of the track (counting from the entrance of the end box) were removed before analyses. Linearized rate maps were made by plotting firing rate along the remaining track with a bin size of 5 cm. Smoothing was applied by a Gaussian kernel with an SD of 10 cm.

Cells were identified using a manual graphical cluster cutting program with 2D projections of the multidimensional parameter space consisting of waveform amplitudes. Putative interneurons (based on waveform width and firing rates) were excluded from further analyses. The range of simultaneously recorded place cells was 1–11, with a median of 2 for both the light and the dark condition.

Identification of Place Cells on the Linear Track. Place cells on the linear track were identified from smoothed rate maps by first estimating the peak rate of the cell, defined as the firing rate in the bin with the highest rate on the linear track. Any continuous region of at least three bins (15 cm) where the firing rate was above 20% of the cell's peak firing rate was then defined as a preliminary field. Final place fields were then calculated by extending the preliminary field successively across bins from each end, starting from the bin that passed 20% of the cell's peak rate, until a bin was reached where the firing rate was again higher than the preceding bin, or the rate was lower than 1% of the peak rate. Fields with fewer than 30 spikes in total were excluded from the analyses. Only place cells with accepted firing fields on all three recording trials were considered for further analysis. Epochs with running speed below 5 cm/s or above 200 cm/s (tracking artifacts) were discarded.

Spatial information content, in bits per spike, was calculated for each rate map as

$$\text{information content} = \sum_i p_i \frac{\lambda_i}{\lambda} \log_2 \frac{\lambda_i}{\lambda},$$

where λ_i is the mean firing rate of a unit in the i-th bin, λ is the overall mean firing rate, and p_i is the probability of the animal being in the i-th bin (occupancy in the i-th bin per total recording time) (25). Cells that passed criteria for place cells were sorted by spatial information content to obtain a systematic measure of the quality of the place fields.

Population Vector Analyses. For all place cells, we constructed stacks of rate maps where x is the spatial dimension (40 bins for the 200-cm linear track) and y is the cell-identity index (Fig. 3). For the first 200-cm trial, cells in the stack were sorted according to the position of the first place field from the left, such that place fields on the beginning of the track were at the top of the plot and place fields at the end were at the bottom. For the middle trial, with shorter tracks, the rate maps were aligned from either the start position or the end position. Firing rates from all recorded cells (population vectors) were then defined for individual bins of the full-length track as well as the short-length track, and corresponding bins (e.g., with similar distance from the start or end of the track) were correlated, yielding a cross-correlation matrix consisting of correlation values for all combinations of bins on the long and short tracks (Fig. 4). All of these population vector correlations were based on unsmoothed rate maps.

Cross-correlation values were compared with chance levels based on a shuffling procedure where, for each cell, the rate map along the full-length track was displaced by a randomly selected number of bins, with the displaced map wrapped around from the end of the track to the beginning. Displacements were selected independently for each cell. Based on the randomly displaced rate maps, population vectors were defined for each bin of the long track. These vectors were correlated with the original vectors for the short track, and a matrix of correlations was generated. The procedure was repeated 1,000 times, yielding a distribution of 1,000 correlation values for each bin of the matrix. For each bin of the original correlation matrix, we then determined the location of the observed value compared with the distribution of correlations for the same bin from the shuffled control data. The analysis identified values of the matrix that exceeded the 95th percentile level of the control distributions.

In a second analysis, we determined how much the cross-correlation matrix for long versus short tracks was displaced compared with an autocorrelation matrix generated from the short-track data alone. The cross-correlogram for long versus short tracks was shifted in a bin-by-bin manner to obtain the displacement along the track that yielded the maximum correlation with the autocorrelation matrix. Only the lower part of the cross-correlation matrix, corresponding to the length of the short track, was considered for this displacement analysis (the upper part of the cross-correlation matrix did not have matching data on the short track). If place field locations were determined exclusively by distance from the starting position, no displacement would be expected (maximum correlations would be obtained as in the autocorrelation matrix). If place fields moved forward relative to the starting position, due to the influence of external stationary cues, a left-to-right cross-correlation-to-autocorrelation displacement would be expected.

Open Field Recordings. Thirteen animals with implants in the hippocampus were tested on three consecutive 15-min trials in a 90 cm × 50 cm cylinder. The middle trial was recorded in complete darkness, with the experimenter remotely controlling the light from outside the recording room. The cylinder walls were covered by black adhesive plastic and a white adhesive plastic cue card (40 cm × 50 cm) on one side of the box.

Analyses of Spike and Position Data in Open Field. The number of spikes and time spent in each 2.5 cm × 2.5 cm bin were counted to make firing rate distributions for each cell. In addition, the position data were smoothed using a Gaussian kernel with an SD of 10 cm.

Analyses of Place Cells in Open Field Experiments. Cells were classified as place cells if their spatial information content exceeded chance levels, determined from a shuffling procedure. The data were shuffled 500 times. Random permutations were generated by time-shifting the entire sequence of spikes fired by a given cell along the animal's path by a random interval between 20 s and the total trial length minus 20 s, with the end of the trial being wrapped to the beginning. For each permutation, a rate map was generated and spatial information content (25) determined, as in the linear track experiments. Place cells were required to pass a mean firing rate of above 0.2 Hz on the first and last trial in the illuminated recording room to be included in the analyses.

Histology. After the last recording day, tetrodes were not moved further. The rats were anesthetized with 5% isoflurane vapor, after which they received an overdose of pentobarbital. After breathing had stopped and animals were unresponsive to tail and pinch reflexes, they were perfused with intracardial saline followed by 4% formaldehyde. The electrodes were kept in the brain for 1–2 h after perfusion. Brains were stored in formaldehyde for at least 48 h before being quickly frozen and cut in 30-μm coronal slices, mounted on glass, and colored with cresyl violet. Recording positions were estimated from digital images of the slices based on final tetrode positions and the turning protocol from the experiments.

Approvals. Experiments were performed in accordance with the Norwegian Animal Welfare Act and the European Convention for the Protection of Vertebrate Animals Used for Experimental and Other Scientific Purposes (permit numbers 3287 and 6173).

ACKNOWLEDGMENTS. We thank V. Frolov for programming; M. P. Witter for advice on histology, and A. M. Amundsgård, K. Haugen, K. Jenssen, E. Kråkvik, and H. Waade for technical assistance. This work was supported by the Kavli Foundation, a student research grant from the Faculty of Medicine at the Norwegian University of Science and Technology, an Advanced Investigator grant from the European Research Council ("ENSEMBLE" Grant 268598), and the Centre of Excellence scheme and the National Infrastructure scheme of the Research Council of Norway (Centre for Neural Computation Grant 223262; NORBRAIN1 Grant 197467).

1. McNaughton BL, Battaglia FP, Jensen O, Moser EI, Moser MB (2006) Path integration and the neural basis of the 'cognitive map'. *Nat Rev Neurosci* 7:663–678.
2. Solstad T, Moser EI, Einevoll GT (2006) From grid cells to place cells: A mathematical model. *Hippocampus* 16:1026–1031.
3. Wills TJ, Cacucci F, Burgess N, O'Keefe J (2010) Development of the hippocampal cognitive map in preweanling rats. *Science* 328:1573–1576.
4. Langston RF, et al. (2010) Development of the spatial representation system in the rat. *Science* 328:1576–1580.
5. Bjerknes TL, Moser EI, Moser MB (2014) Representation of geometric borders in the developing rat. *Neuron* 82:71–78.
6. Muessig L, Hauser J, Wills TJ, Cacucci F (2015) A developmental switch in place cell accuracy coincides with grid cell maturation. *Neuron* 86:1167–1173.
7. Hafting T, Fyhn M, Molden S, Moser MB, Moser EI (2005) Microstructure of a spatial map in the entorhinal cortex. *Nature* 436:801–806.
8. Mittelstaedt ML, Mittelstaedt H (1980) Homing by path integration in a mammal. *Naturwissenschaften* 67:566–567.
9. Müller M, Wehner R (1988) Path integration in desert ants, Cataglyphis fortis. *Proc Natl Acad Sci USA* 85:5287–5290.
10. Etienne AS, Jeffery KJ (2004) Path integration in mammals. *Hippocampus* 14:180–192.
11. Kropff E, Carmichael JE, Moser MB, Moser EI (2015) Speed cells in the medial entorhinal cortex. *Nature* 523:419–424.
12. McNaughton BL, Barnes CA, O'Keefe J (1983) The contributions of position, direction, and velocity to single unit activity in the hippocampus of freely-moving rats. *Exp Brain Res* 52:41–49.
13. Czurkó A, Hirase H, Csicsvari J, Buzsáki G (1999) Sustained activation of hippocampal pyramidal cells by 'space clamping' in a running wheel. *Eur J Neurosci* 11:344–352.
14. Ranck JB (1985) Head direction cells in the deep cell layer of dorsal presubiculum in freely moving rats. *Electrical Activity of the Archicortex*, eds Buzsáki G, Vanderwolf CH (Akademiai Kiado, Budapest), pp 217–220.
15. Taube JS, Muller RU, Ranck JB, Jr (1990) Head-direction cells recorded from the postsubiculum in freely moving rats. I. Description and quantitative analysis. *J Neurosci* 10:420–435.
16. Sargolini F, et al. (2006) Conjunctive representation of position, direction, and velocity in entorhinal cortex. *Science* 312:758–762.
17. O'Keefe J, Burgess N (1996) Geometric determinants of the place fields of hippocampal neurons. *Nature* 381:425–428.
18. Barry C, Hayman R, Burgess N, Jeffery KJ (2007) Experience-dependent rescaling of entorhinal grids. *Nat Neurosci* 10:682–684.
19. Stensola H, et al. (2012) The entorhinal grid map is discretized. *Nature* 492:72–78.
20. Gothard KM, Skaggs WE, McNaughton BL (1996) Dynamics of mismatch correction in the hippocampal ensemble code for space: Interaction between path integration and environmental cues. *J Neurosci* 16:8027–8040.
21. Redish AD, Rosenzweig ES, Bohanick JD, McNaughton BL, Barnes CA (2000) Dynamics of hippocampal ensemble activity realignment: Time versus space. *J Neurosci* 20: 9298–9309.
22. Ravassard P, et al. (2013) Multisensory control of hippocampal spatiotemporal selectivity. *Science* 340:1342–1346.
23. Chen G, King JA, Burgess N, O'Keefe J (2013) How vision and movement combine in the hippocampal place code. *Proc Natl Acad Sci USA* 110:378–383.
24. Aghajan ZM, et al. (2015) Impaired spatial selectivity and intact phase precession in two-dimensional virtual reality. *Nat Neurosci* 18:121–128.
25. Skaggs WE, McNaughton BL, Gothard KM, Markus EJ (1993) An information-theoretic approach to deciphering the hippocampal code. *Advances in Neural Information Processing Systems*, eds Hanson SJ, Cowan JD, Giles CL (Morgan Kaufmann, San Mateo, CA), Vol 5, pp 1030–1037.
26. Resnik E, McFarland JM, Sprengel R, Sakmann B, Mehta MR (2012) The effects of GluA1 deletion on the hippocampal population code for position. *J Neurosci* 32: 8952–8968.
27. Acharya L, Aghajan ZM, Vuong C, Moore JJ, Mehta MR (2016) Causal influence of visual cues on hippocampal directional selectivity. *Cell* 164:197–207.
28. Pastalkova E, Itskov V, Amarasingham A, Buzsáki G (2008) Internally generated cell assembly sequences in the rat hippocampus. *Science* 321:1322–1327.
29. MacDonald CJ, Lepage KQ, Eden UT, Eichenbaum H (2011) Hippocampal "time cells" bridge the gap in memory for discontiguous events. *Neuron* 71:737–749.
30. MacDonald CJ, Carrow S, Place R, Eichenbaum H (2013) Distinct hippocampal time cell sequences represent odor memories in immobilized rats. *J Neurosci* 33:14607–14616.
31. Kraus BJ, Robinson RJ, 2nd, White JA, Eichenbaum H, Hasselmo ME (2013) Hippocampal "time cells": Time versus path integration. *Neuron* 78:1090–1101.
32. Stemmler M, Mathis A, Herz AVM (2015) Connecting multiple spatial scales to decode the population activity of grid cells. *Sci Adv* 1:e1500816.